

Feature robustness and sex differences in medical imaging: a case study in MRI-based Alzheimer's disease detection

Eike Petersen¹, Aasa Feragen¹, Luise da Costa Zemsch¹, Anders Henriksen¹, Oskar Eiler Wiese Christensen¹, and Melanie Ganz^{2,3} for the Alzheimers Disease Neuroimaging Initiative*

¹ Technical University of Denmark, DTU Compute, Kgs. Lyngby, Denmark
 ewipe@dtu.dk

² Neurobiology Research Unit, Rigshospitalet, Copenhagen, Denmark

³ University of Copenhagen, Department for Computer Science, Copenhagen, Denmark

Abstract. Convolutional neural networks have enabled significant improvements in medical image-based disease classification. It has, however, become increasingly clear that these models are susceptible to performance degradation due to spurious correlations and dataset shifts, which may lead to underperformance on underrepresented patient groups, among other problems. In this paper, we compare two classification schemes on the ADNI MRI dataset: a very simple logistic regression model that uses manually selected volumetric features as inputs, and a convolutional neural network trained on 3D MRI data. We assess the robustness of the trained models in the face of varying dataset splits, training set sex composition, and stage of disease. In contrast to earlier work on diagnosing lung diseases based on chest x-ray data, we do not find a strong dependence of model performance for male and female test subjects on the sex composition of the training dataset. Moreover, in our analysis, the low-dimensional model with manually selected features outperforms the 3D CNN, thus emphasizing the need for automatic robust feature extraction methods and the value of manual feature specification (based on prior knowledge) for robustness.

Keywords: Deep Learning · MRI · Alzheimer's Disease · Robustness

1 Introduction

In recent years, various groups have reported highly accurate detection of Alzheimer's disease (AD) and progressive mild cognitive impairment (pMCI) – which represents an earlier disease stage that continues to progress into AD

* Data used in preparation of this article was obtained from the Alzheimers Disease Neuroimaging Initiative (ADNI) database (<http://www.adni-info.org/>). The investigators within the ADNI contributed to the design and implementation of ADNI and/or provided data, but did not participate in analysis or writing of this report.

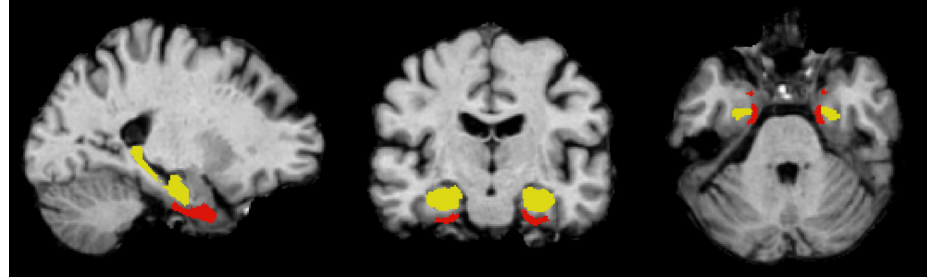


Fig. 1. Slices of an exemplary recording used in this study, skull-stripped and registered to a common space. Hippocampus and entorhinal cortex (yellow and red, segmented using FreeSurfer) are highlighted. Left to right: sagittal, coronal, and axial view.

or other types of dementia [16] – based on MRI volumes using convolutional neural networks (CNNs) [25]. At the same time, the potential brittleness of deep learning has become apparent due to issues like model underspecification [8], spurious correlations [12], and susceptibility to dataset shift [5]. Multiple reviews in the medical domain have shown that deep learning-based publications often suffer from inadequate model reporting and overly optimistic performance estimates [14,26]. Wen et al. [25] found in their systematic review that half of the studies reporting on MRI-based AD detection using deep learning potentially suffered from data leakage, likely leading to inflated performance estimates. Additionally, in clinical applications with low-dimensional input spaces, several systematic reviews have found no performance benefit of machine learning-based techniques over simple logistic regression [7,17], thus raising the question of whether simple approaches based on manually extracted, low-dimensional features may also perform competitively in the medical imaging domain.

In a parallel development, the question of sex and gender-related performance disparities of machine learning models has lately received a lot of attention [18,22]. Studies have shown that CNNs can accurately identify a patient’s age, sex, and ethnicity from chest x-ray images [6,27], and that chest x-ray classifiers tend to underdiagnose underserved patient populations [22]. Larrazabal et al. [15] have analyzed the effect of training dataset sex imbalance on a chest x-ray classifier’s performance for male and female subgroups, finding a consistent decrease in performance for the underrepresented sex. To the authors’ knowledge, similar analyses have yet to be performed in the brain MRI classification setting, even though it is known that AD presents differently in males and females [16].

Training on a sex-imbalanced dataset and then evaluating model performance on the underrepresented group represents a particular type of *dataset shift* [21], and the close connection between model robustness (to dataset shift and other challenges) and algorithmic fairness has been emphasized recently [2]. To achieve robustness to dataset shifts, the *feature space* in which classification is performed plays a crucial role: to be robust against dataset shifts, estimation must be performed in a feature space that gives rise to a classifier that is optimal across

Table 1. Composition of the dataset used in this study (based on the ADNI dataset [13]), stratified by sex and recording field strength.

Diagnosis	Male	Female	1.5 T	3 T	Total
AD	181 (54.03%)	154 (45.97%)	175 (52.24%)	160 (47.76%)	335
HC	282 (43.52%)	366 (56.48%)	219 (33.80%)	547 (66.20%)	648
pMCI	149 (58.66%)	105 (41.34%)	184 (72.44%)	70 (27.56%)	254
sMCI	155 (59.62%)	105 (40.38%)	122 (46.92%)	138 (53.08%)	260

different environments [3]. This feature space can, of course, either be manually crafted or automatically inferred, as is usually the case in deep learning [1].

In this paper, we analyze the robustness of two different MRI volume-based classifiers to distribution shifts. Both classifiers are trained to detect Alzheimer’s disease, based on different feature representations. The first is a very simple logistic regression model that uses manually selected volumetric features as inputs, which are obtained using standard MRI processing tools [4,11]. The second is a CNN using the full 3D MRI volumes as inputs. For analyzing the classifiers’ robustness, we consider two separate types of distribution shifts: Firstly, we analyze the effect of differing training dataset sex compositions on the performance for male and female test subjects, similar to the analysis of Larrazabal et al. [15]. And secondly, like various other groups have done [25] (although not combined with the sex imbalance analysis we perform), we evaluate the performance of classifiers trained on subjects diagnosed with AD and healthy controls on a test set consisting of subjects with stable and progressive MCI.

2 Methods

2.1 Dataset

We use MRI volumes from the ADNI dataset [13] (700, 463, and 334 recordings from ADNI1, ADNI2, and ADNI3, respectively), including a single T1-weighted structural MRI volume (acquired on different MR scanners using a field strength of either 1.5 T or 3 T) per subject in our experiments. Like various other studies [25], we consider two groups of subjects, giving rise to two classification tasks: firstly, healthy control (HC) and Alzheimer’s disease (AD) subjects and, secondly, stable and progressive mild cognitive impairment (sMCI, pMCI) subjects. Subjects were labeled as pMCI in our analysis if they were diagnosed with MCI at the time of the recording and then were diagnosed with AD at any point during the following five years.¹ Subjects were labeled as sMCI if they were diagnosed with MCI at the time of the recording, not diagnosed with AD at any point during the five-year follow-up period, and if there was at least one valid diagnosis from

¹ This definition only encompasses (progressive) *amnestic* MCI, since non-amnestic MCI may develop into non-AD dementias [16].

years three to five after the initial recording was made. Table 1 summarizes the dataset used in our study.

2.2 AD Classification using logistic regression

Extraction of hippocampal volume (HCV) and entorhinal cortex volume (ECV) from MRI volumes was performed using FreeSurfer v7.1.1[11], see fig. 1 for an example. Intracranial volume (ICV) was calculated using SPM12 [4].

A simple logistic regression (LR) model of the form

$$P(\text{AD}) \approx q_{\text{AD}} = \sigma(\theta_1 \cdot \text{Age} + \theta_2 \cdot \text{ICV} + \theta_3 \cdot \text{HCV} + \theta_4 \cdot \text{ECV}), \quad (1)$$

with $\sigma(\cdot)$ denoting the sigmoid function, was fitted using stochastic gradient descent for 4000 epochs (initial learning rate 10^{-3} , automatic learning rate scheduling – if there is no improvement in the validation loss for 10 epochs, the learning rate is halved –, momentum 0.9, early stopping based on the validation loss, batch size 256). The loss function was binary cross-entropy with L_2 regularization (regularization constant 10^{-4}).

2.3 AD Classification using CNNs

The subject-specific MRI images were skull-stripped and registered to a common space (MNI305) using FreeSurfer v7.1.1[11], resulting in spatially normalized grayscale volumes of the dimensionality $256 \times 256 \times 256 \text{ mm}^3$, which are then cropped to include the whole brain ($186 \times 186 \times 191 \text{ mm}^3$).

Dataset augmentation was performed to increase model robustness and effective training dataset size. Whenever a training sample was drawn during model training, in 80% of the cases, it was transformed using one (randomly selected) of nine 3D image transformations implemented in the torchio library [20]: rotation, elastic deformation, flipping, blurring, addition of Gaussian noise, addition of an MRI bias field, spike, ghosting, or motion artifact.

A convolutional neural network (CNN) was trained, using the preprocessed 3D MRI volumes as inputs and the subject’s AD/HC label as the target. The model architecture was inspired by the structure used by Tinauer et al. [23] and was (manually) selected based on validation set performance. The convolutional part of the model consists of eight consecutive convolution layers (all with sixteen channels), each followed by a rectified linear unit (ReLU). The first two layers use kernels of size $5 \times 5 \times 5$; the subsequent six layers use $3 \times 3 \times 3$ kernels. Every second layer uses a stride of two, thus progressively reducing image resolution. The convolutional part of the model is followed by a dropout layer ($p = 0.5$), a fully connected linear layer with 32 output channels, a ReLU, another dropout layer ($p = 0.5$), and the final, fully connected classification layer (followed by a sigmoid activation function). The model has 337,000 trainable parameters, which are estimated using the Adam optimization algorithm (initial learning rate 10^{-4} , automatic learning rate scheduling based on the validation loss as described above, 200 epochs, batch size 6, early stopping based on the validation loss) to minimize binary cross-entropy (no regularization).

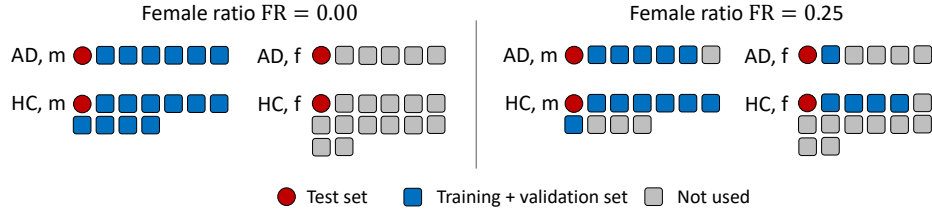


Fig. 2. Visualization of the AD/HC dataset and two exemplary splits. Each marker represents 25 subjects (rounded). For clarity, only one of the five test sets and only two of the five training and validation datasets for this test set (all with different male–female ratios $FR = \frac{n_f}{n_f + n_m}$, with n_f and n_m the number of females and males in the combined training and validation dataset) are shown.

2.4 Performance and robustness evaluation

To evaluate the two models' overall performance and robustness, we trained them on 125 (LR) and 25 (CNN) different training datasets and evaluated them on six different test sets. First, five AD/HC test sets of size 100 were selected with 25 samples each of male/female AD/HC subjects. There was no subject overlap between the five test sets. Next, for each test set, five combined training and validation sets of size 400 were drawn from the remaining AD/HC subjects (without replacement), stratified by the disease label and with five different male-to-female ratios (0% to 100% females in 25% steps). Subjects were reused where possible to minimize training dataset variation between the different sex ratio conditions, i.e., female subjects used at a female ratio (FR) of 50% represented a subset of female subjects used at an FR of 75%, and equivalently for other FRs and male subjects. Each combined training and validation set was then split randomly into five folds following standard recommendations for neuroimaging [24]. For the logistic regression, each fold was used once as the validation set, resulting in a total of five training-validation set combinations per test set (of which there are five) and sex ratio (of which there are five), yielding a total of 125 different training and validation datasets. For the CNNs, because of the computational effort required for training, only one (randomly selected) of the five fold combinations was used per sex ratio, thus yielding a total of 25 different training and validation datasets. Each model was then evaluated on both the respective AD/HC test set and the full sMCI/pMCI dataset (which had not been used for training), calculating performance metrics on both males and females. Figure 2 illustrates the full AD/HC dataset and two exemplary data splits.

The decision thresholds for all models were set by selecting the threshold maximizing the geometric mean of sensitivity and specificity on the validation dataset, a standard method in the imbalanced classification domain [10]. All models were implemented and trained using PyTorch Lightning v.1.5.9 [9] and training one CNN took about twelve hours on a single NVIDIA Titan X GPU. When the performance of models trained on the same datasets was compared, statistical significance was assessed using Wilcoxon signed-rank tests.

3 Results

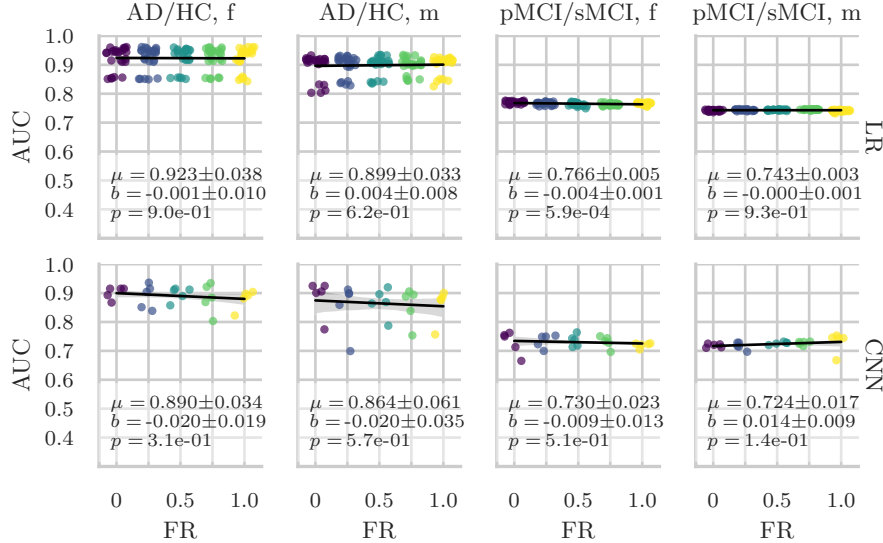
Figure 3 shows the distribution of the area under the curve (AUC) of the receiver-operating characteristic and the accuracy (ACC) achieved by the trained models on the different test sets. To assess the dependence of model performance for males and females on the training dataset sex composition, regression lines were fit and a t-test was performed to assess whether the slope was significantly different from zero. As expected, and as found in previous studies [25], both models show a significant performance drop on the sMCI vs. pMCI classification task, as opposed to HC vs. AD classification, which they were trained on. The LR model achieves consistently high AUC and ACC across all training and validation sets, and performance is similar for male and female test subjects, although significantly better for females ($p = 2.7 \times 10^{-5}$ and $p = 3.0 \times 10^{-22}$ for AUC on AD/HC and pMCI/sMCI, respectively). For the LR model, all identified slopes were small (< 0.004) and non-significant ($p \gg 0.05$) in all cases except female pMCI/sMCI subjects, where $p = 0.00059$. The CNN performed significantly worse compared to the LR ($p = 9.7 \times 10^{-12}$ for AUC, $p = 3.9 \times 10^{-4}$ for ACC), and it exhibited a stronger dependence of performance for male and female test subjects on the training dataset composition (as indicated by larger slope values b in fig. 3), although in all cases except male pMCI/sMCI subjects this was not statistically significant ($p \gg 0.05$).

4 Discussion & conclusion

In the present study, motivated by recent work demonstrating performance disparities in medical image classifiers between patient populations [15,22], we have analyzed the robustness of two brain MRI classifiers and their associated feature representations to multiple types of distribution shift. We analyzed the effect of different ratios of male and female examples in the training dataset on the performance of the trained classifier for male and female test subjects. Logistic regression using manually extracted volumetric features was compared to a standard 3D CNN classifier using the full 3D MRI volumes as inputs, with both models performing within the range reported in the review of Wen et al. [25] for studies without suspected data leakage. As opposed to a previous study on lung disease detection from chest x-ray data [15], we found only a weak dependence of classifier performance for male and female test subjects on the training dataset sex composition. In our study, the LR model, using manually selected volumetric features, performed significantly better on average than a 3D CNN using the full MRI images. While this might change for larger dataset sizes, our sample size is comparable to typical sample sizes used in this domain.

The small effect of the training dataset sex composition observed in our study is in line with previous research showing sex-related differences in MRI recordings to be limited and gradual [28], as opposed to the apparent sex differences in chest x-ray recordings. Nevertheless, it is an important result that – despite known sex differences in AD [16] – the training dataset composition does not appear to

(A)



(B)

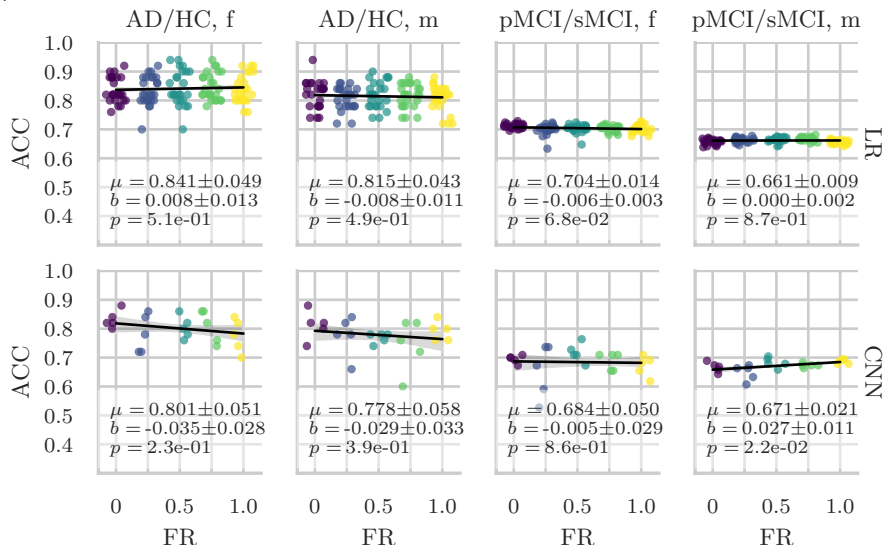


Fig. 3. Distribution of (A) the area under the curve (AUC) of the receiver-operating characteristic and (B) the accuracy achieved by the trained models (first row in both panels: LR, second row: CNN) on the different test sets. FR: ratio of female subjects in the training and validation set, μ : average AUC / ACC (\pm standard deviation) across all sex ratios, b : slope of the regression line (\pm standard deviation), p -value null hypothesis: $b = 0$. Random jitter is added to all x coordinates to prevent excessive overlap – all points are sampled at $FR \in \{0, 0.25, 0.5, 0.75, 1.0\}$, as indicated by the five different colors. Note the truncation of all y-axes.

have a strong effect on male and female test subject performance, indicating that the employed feature representations are – to some degree, at least – invariant to this dataset shift [3].

One potential limitation of our study concerns the preprocessing employed for both models. The employed segmentation steps are partially based on MRI atlases, which have been extracted from study databases. Thus, even in the cases in which the training dataset nominally contained no males or no females, this preprocessing step still incorporated some information about male and female subjects. The degree to which this influenced the results of our analyses is challenging to quantify, but it represents a potentially confounding factor that might cause an underestimation of the effect of the training dataset composition on the performance of LR and CNN models for male and female test subjects. Practical applications, however, typically also employ atlas-based preprocessing steps, and thus our analysis is closer to practical application scenarios than if we had omitted these preprocessing steps.

An important avenue for future research concerns the question of whether environment-invariant feature representations can be inferred automatically; an end towards which various methods have been proposed [3,19,29]. This would potentially allow for mitigating the effect of training dataset composition on male and female test subject performance in domains with substantial dataset shifts, such as chest x-ray analysis. Even in the brain MRI analysis domain considered in this contribution, generalization to different populations remains an unsolved problem [25], with important consequences for the general robustness and fairness of the resulting systems.

Code & data availability The full code for all implemented models, dataset splitting, and statistical analyses is available online in our GitHub repository: <https://github.com/to-be-added-after-review>.

Acknowledgements The authors would like to thank Friendly Colleague, Our Institute, or helpful comments on the manuscript and the statistical analysis. This research was supported by A Grant-Giving Institution (grant number 12345). Data collection and sharing for this project was funded by the ADNI (National Institutes of Health Grant U01 AG024904). ADNI is funded by the National Institute on Aging, the National Institute of Biomedical Imaging and Bioengineering, and through generous contributions from private sector institutions. The Canadian Institutes of Health Research is providing funds to support ADNI clinical sites in Canada. Private sector contributions are facilitated by the Foundation for the National Institutes of Health (www.fnih.org). The grantee organization is the Northern California Institute for Research and Education, and the study is coordinated by the Alzheimer’s Disease Cooperative Study at the University of California, San Diego. ADNI data are disseminated by the Laboratory for Neuro Imaging at the University of California, Los Angeles.

References

1. Abrol, A., Fu, Z., Salman, M., Silva, R., Du, Y., Plis, S., Calhoun, V.: Deep learning encodes robust discriminative neuroimaging representations to outperform standard machine learning. *Nature Communications* **12**(1) (2021). <https://doi.org/10.1038/s41467-020-20655-6>
2. Adragna, R., Creager, E., Madras, D., Zemel, R.: Fairness and robustness in invariant learning: A case study in toxicity classification. In: NeurIPS Workshop on Algorithmic Fairness through the Lens of Causality and Interpretability (2020), <https://arxiv.org/abs/2011.06485>
3. Arjovsky, M., Bottou, L., Gulrajani, I., Lopez-Paz, D.: Invariant risk minimization. arXiv (2019), <https://arxiv.org/abs/1907.02893>
4. Ashburner, J.: SPM: a history. *Neuroimage* **62**(2), 791–800 (2012). <https://doi.org/10.1016/j.neuroimage.2011.10.025>
5. Azulay, A., Weiss, Y.: Why do deep convolutional networks generalize so poorly to small image transformations? *Journal of Machine Learning Research* **20**(184), 1–25 (2019), <http://jmlr.org/papers/v20/19-519.html>
6. Banerjee, I., Bhimireddy, A.R., Burns, J.L., Celi, L.A., Chen, L.C., Correa, R., et al.: Reading race: AI recognises patient's racial identity in medical images. arXiv (2021), <https://arxiv.org/abs/2107.10356>
7. Cowling, T.E., Cromwell, D.A., Bellot, A., Sharples, L.D., van der Meulen, J.: Logistic regression and machine learning predicted patient mortality from large sets of diagnosis codes comparably. *Journal of Clinical Epidemiology* **133**, 43–52 (2021). <https://doi.org/10.1016/j.jclinepi.2020.12.018>
8. D'Amour, A., Heller, K., Moldovan, D., Adlam, B., Alipanahi, B., Beutel, A., et al.: Underspecification presents challenges for credibility in modern machine learning. CoRR (2020), <https://arxiv.org/abs/2011.03395>
9. Falcon, W., the PyTorch Lightning team: PyTorch Lightning (version 1.5.9) (2019), <https://www.pytorchlightning.ai>
10. Fernández, A., García, S., Galar, M., Prati, R.C., Krawczyk, B., Herrera, F.: Performance measures. In: Learning from Imbalanced Data Sets, pp. 47–61. Springer International Publishing (2018). https://doi.org/10.1007/978-3-319-98074-4_3
11. Fischl, B.: Freesurfer. *Neuroimage* **62**(2), 774–781 (2012). <https://doi.org/10.1016/j.neuroimage.2012.01.021>
12. Geirhos, R., Jacobsen, J.H., Michaelis, C., Zemel, R., Brendel, W., Bethge, M., Wichmann, F.A.: Shortcut learning in deep neural networks. *Nature Machine Intelligence* **2**(11), 665–673 (2020). <https://doi.org/10.1038/s42256-020-00257-z>
13. Jack, C.R., Bernstein, M.A., Fox, N.C., Thompson, P., Alexander, G., Harvey, D., et al.: The Alzheimer's disease neuroimaging initiative (ADNI): MRI methods. *Journal of Magnetic Resonance Imaging* **27**(4), 685–691 (2008). <https://doi.org/10.1002/jmri.21049>
14. Jacobucci, R., Littlefield, A.K., Millner, A.J., Kleiman, E.M., Steinley, D.: Evidence of inflated prediction performance: A commentary on machine learning and suicide research. *Clinical Psychological Science* **9**(1), 129–134 (2021). <https://doi.org/10.1177/2167702620954216>
15. Larrazabal, A.J., Nieto, N., Peterson, V., Milone, D.H., Ferrante, E.: Gender imbalance in medical imaging datasets produces biased classifiers for computer-aided diagnosis. *Proceedings of the National Academy of Sciences* **117**(23), 12592–12594 (2020). <https://doi.org/10.1073/pnas.1919012117>

16. Mielke, M., Vemuri, P., Rocca, W.: Clinical epidemiology of Alzheimer's disease: assessing sex and gender differences. *Clinical Epidemiology* p. 37 (2014). <https://doi.org/10.2147/cepi.s37929>
17. Nusinovici, S., Tham, Y.C., Yan, M.Y.C., Ting, D.S.W., Li, J., Sabanayagam, C., et al.: Logistic regression was as good as machine learning for predicting major chronic diseases. *Journal of Clinical Epidemiology* **122**, 56–69 (2020). <https://doi.org/10.1016/j.jclinepi.2020.03.002>
18. Obermeyer, Z., Powers, B., Vogeli, C., Mullainathan, S.: Dissecting racial bias in an algorithm used to manage the health of populations. *Science* **366**(6464), 447–453 (2019). <https://doi.org/10.1126/science.aax2342>
19. Pawłowski, N., Castro, D.C., Glocker, B.: Deep structural causal models for tractable counterfactual inference. In: *Advances in Neural Information Processing Systems*. vol. 33, pp. 857–869. Curran Associates, Inc. (2020), <https://proceedings.neurips.cc/paper/2020/file/0987b8b338d6c90bbedd8631bc499221-Paper.pdf>
20. Pérez-García, F., Sparks, R., Ourselin, S.: TorchIO: A python library for efficient loading, preprocessing, augmentation and patch-based sampling of medical images in deep learning. *Computer Methods and Programs in Biomedicine* **208**, 106236 (2021). <https://doi.org/10.1016/j.cmpb.2021.106236>
21. Quiñonero-Candela, J., Sugiyama, M., Lawrence, N.D., Schwaighofer, A.: *Dataset shift in machine learning*. MIT Press (2009)
22. Seyyed-Kalantari, L., Zhang, H., McDermott, M.B.A., Chen, I.Y., Ghassemi, M.: Underdiagnosis bias of artificial intelligence algorithms applied to chest radiographs in under-served patient populations. *Nature Medicine* **27**(12), 2176–2182 (2021). <https://doi.org/10.1038/s41591-021-01595-0>
23. Tinauer, C., Heber, S., Pirpamer, L., Damulina, A., Schmidt, R., Stollberger, R., et al.: Interpretable brain disease classification and relevance-guided deep learning. *medRxiv* (2021). <https://doi.org/10.1101/2021.09.09.21263013>
24. Varoquaux, G., Raamana, P.R., Engemann, D.A., Hoyos-Idrobo, A., Schwartz, Y., Thirion, B.: Assessing and tuning brain decoders: cross-validation, caveats, and guidelines. *NeuroImage* **145**, 166–179 (2017). <https://doi.org/10.1016/j.neuroimage.2016.10.038>
25. Wen, J., Thibeau-Sutre, E., Diaz-Melo, M., Samper-González, J., Routier, A., Bottani, S., et al.: Convolutional neural networks for classification of Alzheimer's disease: Overview and reproducible evaluation. *Medical Image Analysis* **63**, 101694 (2020). <https://doi.org/10.1016/j.media.2020.101694>
26. Wynants, L., Van Calster, B., Collins, G.S., Riley, R.D., Heinze, G., Schuit, E., et al.: Prediction models for diagnosis and prognosis of covid-19: systematic review and critical appraisal. *BMJ* **369**, m1328 (2020). <https://doi.org/10.1136/bmj.m1328>
27. Yi, P.H., Wei, J., Kim, T.K., Shin, J., Sair, H.I., Hui, F.K., et al.: Radiology “forensics”: determination of age and sex from chest radiographs using deep learning. *Emergency Radiology* **28**(5), 949–954 (2021). <https://doi.org/10.1007/s10140-021-01953-y>
28. Zhang, Y., Luo, Q., Huang, C.C., Lo, C.Y.Z., Langley, C., Desrivières, et al.: The human brain is best described as being on a female/male continuum: evidence from a neuroimaging connectivity study. *Cerebral Cortex* **31**(6), 3021–3033 (2021). <https://doi.org/10.1093/cercor/bhaa408>
29. Zhao, Q., Adeli, E., Pohl, K.M.: Training confounder-free deep learning models for medical applications. *Nature Communications* **11**(1) (2020). <https://doi.org/10.1038/s41467-020-19784-9>